2014

Investigation Of The Parameters Affecting Crankshaft And Rotor Interference Fit

Naz?m Arda Eyyubo?lu
Arçelik A.?. Compressor Plant, Turkey, arda.eyyuboglu@arcelik.com

Investigation of the Parameters Affecting Crankshaft and Rotor Interference Fit

Nazım Arda Eyyuboğlu

Arcelik A.S., Compressor R&D Center
Compressor Plant, Organize Sanayi Bolgesi, 1. Cadde, Eskisehir, Turkey
Phone: +90 222 213 46 77, Fax: +90 222 213 43 44, arda.eyyuboglu@arcelik.com

ABSTRACT

In recent years small sized compressors have been introduced to the market, by reducing the height, length and width of the compressor. This improvement allows refrigerator's compressor housing area become smaller; hence cabinet volume of the refrigerator increases. One of the parameters affecting the height of the compressor is the length of interference fit between crankshaft and rotor which is also critical to prevent split off the rotor from crankshaft during operational life. In this study theoretical model is suggested for crankshaft-rotor interference fit phenomenon and it is verified by experimental study. Using this model, parametric study is carried out to determine the minimum possible interference fit length for a given compressor model.

1. INTRODUCTION

The hermetic compressors which are used almost all household refrigeration systems are located at the bottom cabinet of refrigeration volume. Refrigerator designers make bottom cabinet volume as small as possible in order to maximize refrigerator volume. Bottom cabinet volume of the refrigerator is directly related to size of the compressor. Especially bottom cabinet volume of the refrigerator is downscaled by reducing height of the compressor.

There are many factors affect the height of the compressor; such as height of the crankcase or height of the springs. However most effective parameter for height of the compressor is stack height of the stator, because stack height of the stator can vary from 30 mm to 50 mm approximately. In BLDC(brushless DC) stators or stator with outer rotors height value may be less than 30 mm. Therefore minimized height compressors, which are also contain inverter technology, are on the market recently.

In low sized compressor, there is design challenge about rotor interference with crank. Normally the stack height of the rotor equals to the stack height of the stator for effective production and performance. In rotor structure design some portion of height is used for interference fit with crank, remaining part has clearance with crankcase main bearing portion which is seen clearly at
Figure 1. Lengthening crankcase main bearing decreases forces on crankshaft, which can be proven by force analysis of the crankshaft. However there is structural boundary for length of crank case main bearing. This length has to be decrease more and more while stack height of the rotor is downsized. Consequently minimum length has to be chosen for length of interference fit between crank and rotor. Also this length should guarantee to prevent split off the rotor from crank.

The goal of this study is to identify the parameters affecting interference fit forces. In order to analyze interference fit; theoretical, experimental studies are conducted. In theoretical analysis thick walled cylinder theorem is used for calculations. However end conditions do not take into account in theoretical process. In experimental studies torque wrench is used for determining split off torque for interference fit. Finally the results of the theoretical and experimental studies are compared and discussed in last section.

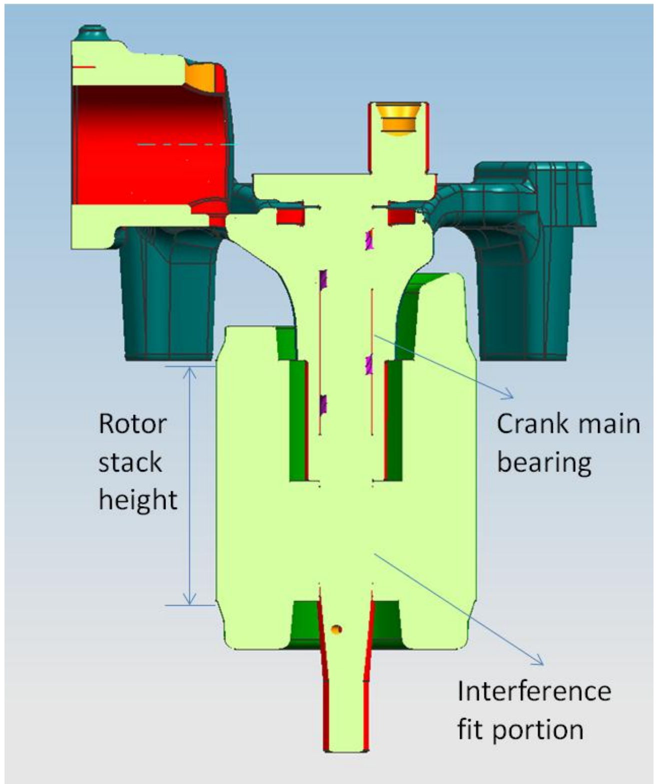

Figure 1: Section view of compressor inner assembly

2. THEORETICAL CALCULATION

When two cylinders attach to each with radial interference, there is pressure developed according to thick wall cylinder theory. In compressor design always crank main bearing diameter is bigger than rotor shaft hole in order support radial interference force. In thick cylinder theory radial and tangential stress are showed in Equation (1) and Equation (2) (Budynas, 1999) (by using polar coordinate system). This theorem is valid when the cylinder axisymmetric about z axis.

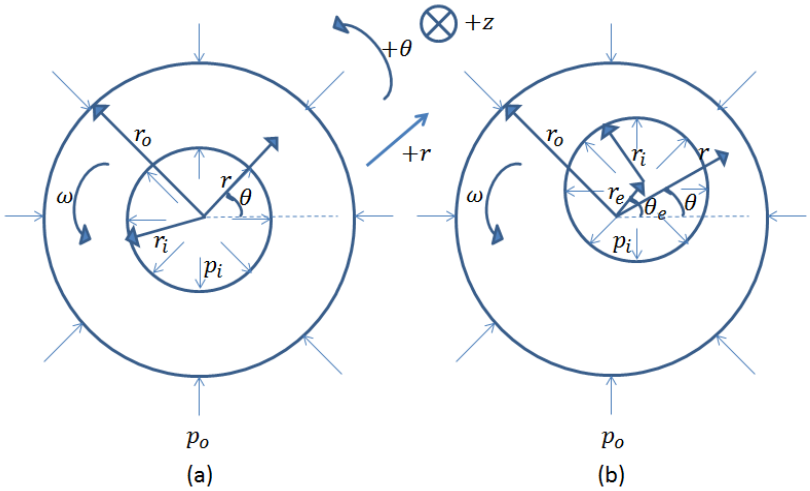

Figure 2: Thick walled pressurized cylinder. (a) axisymmetric rotating cylinder (b) asymmetric rotating cylinder

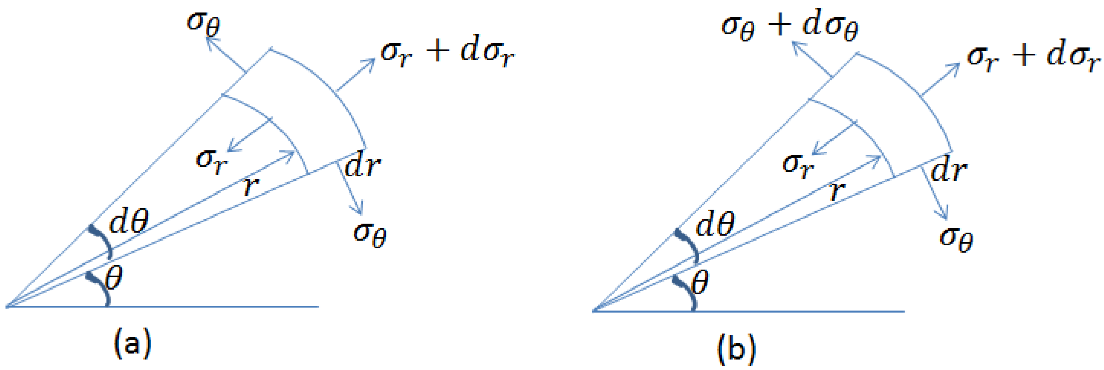

Figure 3: Infinitesimal element for cylinder. (a) axisymmetric cylinder, (b) asymmetric cylinder

$$r\frac{d^2\sigma_r}{dr^2} + 3\frac{d\sigma_r}{dr} = -(3+\vartheta)\rho\omega^2 r \tag{1}$$

$$\sigma_\theta = r\frac{d\sigma_r}{d_r} + \sigma_r + \rho\omega^2 r^2 \tag{2}$$

The Equation (1) can be solved by using differential equation techniques as follows

$$\sigma_r = C_1 + \frac{C_2}{r^2} - \frac{3+\vartheta}{8}\rho\omega^2 r^2 \tag{3}$$

By substituting σ_r in Equation (2) from Equation (3), σ_θ can be written as

$$\sigma_\theta = C_1 - \frac{C_2}{r^2} - \frac{1+3\vartheta}{8}\rho\omega^2 r^2 \tag{4}$$

However; lubricating hole at most of cranks are eccentric with respect to outer diameter of crank, which can be seen at Figure 4 . Therefore differential equations must be rewritten for new boundary conditions. Diagraphs for asymmetric case are shown at b part of Figure 2 and Figure 3. Furthermore those equations are contained partial differential equations rather ordinary differential equation. Whereas stress functions, both radial and tangential, are function of radius and angle.

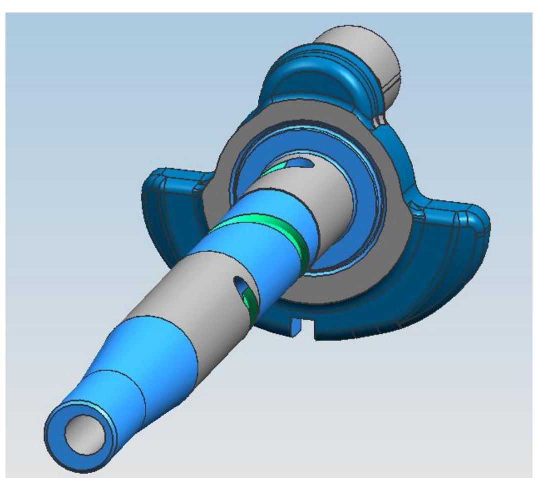

Figure 4: Bottom view of the crank

$$\sum F_r = ma_r = (\rho r d\theta dr dz)(-r\omega^2) = -\rho\omega^2 r^2 d\theta dr dz \quad (5)$$

$$\sum F_r = (\sigma_r + d\sigma_r)(r + dr)d\theta dz - \sigma_r r d\theta dz - (2\sigma_\theta + d\sigma_\theta)\sin\frac{d\theta}{2} dr dz \quad (6)$$

Below equation is drawn from Equation (5) and (6).

$$E\frac{\partial^2 u_\theta}{\partial r \partial \theta} = r\left[\frac{\partial^2 \sigma_r}{\partial r^2} + 3\frac{\partial \sigma_r}{\partial r} + \rho\omega^2 r(3 + \vartheta)\right] \quad (7)$$

Equation (7) is partial differential form of radial stress for asymmetric pressurized cylinder at polar coordinate system. In press fit, inner and outer member surfaces are touched each other after that they are mated at perfect cylinder which has a radius between outer and inner member radius. Therefore at outer surface of inner member there is zero tangential displacement. Furthermore all members of crank are assumed to move in radial direction. Hence derivatives of tangential displacement are also zero. By this assumption Equation (7) is reduced to Equation (1) which is valid for axisymmetric case. Solution of Equation (1) and (2)are given at Equation (3) and (4). In Equation (3) and (4), C_1 and C_2 can be found by applying end conditions for press fit. Additionally free body diagram of crankshaft and rotor is given at Figure 5. In Figure 5 dotted line represents initial state of radius, solid line represents radius after press fitting.

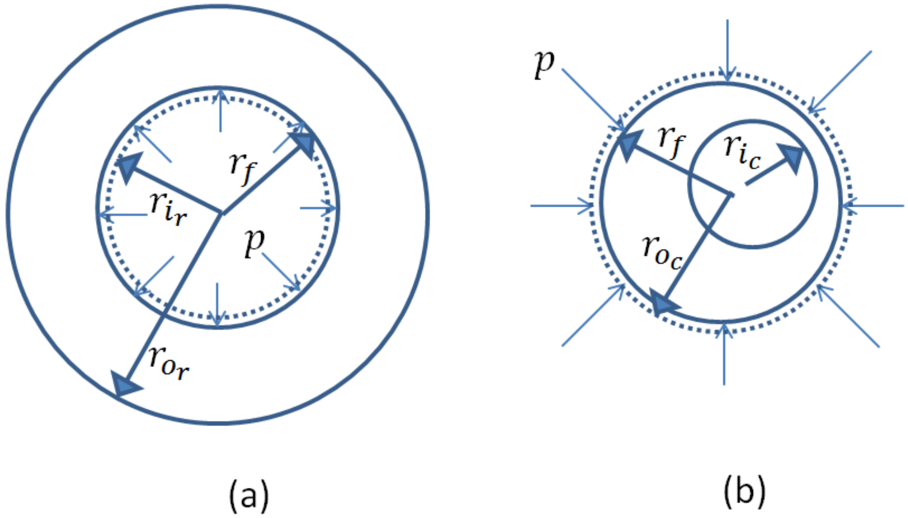

Figure 5: Stress distribution after press fit. (a) rotor, (b) crankshaft

For outer member which is axisymmetric cylinder end conditions are given at Table 1

Table 1: Boundary conditions for rotor

At outer ring	
Position	Radial stress
Inner radius	*-p*
Outer radius	0

By applying these boundary conditions to Equation (3), radial stress equations for inner and outer ring can be showed as follow

$$b = \frac{3+\vartheta}{8}\rho\omega^2 \tag{8}$$

$$\sigma_{rr} = br_o{}^2 - r_i{}^2\left(\frac{p}{r_i{}^2 - r_o{}^2} - b\right) + \frac{r_o{}^2 r_i{}^2}{r^2}\left(\frac{p}{r_i{}^2 - r_o{}^2} - b\right) - br^2 \tag{9}$$

The expression for $c_1$and c_2 can be written at tangential stress equation. b and d terms are used for simplicity of equations

$$d = \frac{1+3\vartheta}{8}\rho\omega^2 \tag{10}$$

$$\sigma_{\theta r} = br_o{}^2 - r_i{}^2\left(\frac{p}{r_i{}^2 - r_o{}^2} - b\right) - \frac{r_o{}^2 r_i{}^2}{r^2}\left(\frac{p}{r_i{}^2 - r_o{}^2} - b\right) - dr^2 \tag{11}$$

For crankshaft boundary conditions at mating face is the same as with outer ring. That is mean that at outer radius of crankshaft radial stress is equal to press fit pressure. However, position of inner radius is changing with respect to θ. The position of inner radius is calculated from geometry, related equation is given at Table 2

Table 2: Boundary conditions for crankshaft

At inner ring	
Position	Radial stress
$r = r_e\cos(\theta-\theta_e) - \sqrt{r_i{}^2 - r_e{}^2\sin^2(\theta-\theta_e)}$	0
Outer radius	*-p*

However equation for inner radius is valid for $r_i > r_e$, otherwise piecewise equation must be written for boundary condition. Radial stress function is given at Equation (12)

$$\sigma_{rc} = \frac{p + b(r_i{}^2 - r_o{}^2)}{\frac{r_i{}^2 - r_o{}^2}{r_o{}^2}} + br_i{}^2 - \frac{p + b(r_i{}^2 - r_o{}^2)}{r^2\frac{r_i{}^2 - r_o{}^2}{r_i{}^2 r_o{}^2}} - br^2 \tag{12}$$

$$\sigma_{\theta c} = \frac{p + b(r_i{}^2 - r_o{}^2)}{\frac{r_i{}^2 - r_o{}^2}{r_o{}^2}} + br_i{}^2 + \frac{p + b(r_i{}^2 - r_o{}^2)}{r^2\frac{r_i{}^2 - r_o{}^2}{r_i{}^2 r_o{}^2}} - dr^2 \tag{13}$$

Actually press fit case consists statically indeterminate equations, because deflection for each member cannot be calculated from free body diagram. Therefore deflection analysis must be used. Radial displacement for each member is:

$$u_r = \frac{r}{E}(\sigma_\theta - \vartheta\sigma_r) \tag{14}$$

Also difference of radial displacement of rotor and crank is equal to radial interference which is known parameter.

$$u_{rr} - u_{rc} = r_c - r_r = \delta \tag{15}$$

After determining radial displacement for each member, they can be subtracted according to Equation (15). Final result is:

$$p = \frac{\delta + 2b_c {r_{ci}}^2 \frac{r_f}{E_c} + \frac{{r_f}^3}{E_c}(b_c - d_c) - 2b_r {r_o}^2 \frac{r_f}{E_r} - \frac{{r_f}^3}{E_r}(b_r - d_r)}{r_f \left[\frac{1}{E_r}\left(\vartheta_r - \frac{{r_{ro}}^2 + {r_f}^2}{{r_f}^2 - {r_{ro}}^2}\right) - \frac{1}{E_c}(\vartheta_c + \frac{{r_{ci}}^2 + {r_f}^2}{{r_{ci}}^2 - {r_f}^2})\right]} \quad (16)$$

Although Equation (16) seems constant, r_i term is function of θ which is shown at Table 2. It is meant that pressure, which develops after press fit operation, is changed at tangential direction. Also Equation (16) is very similar Equation 3-55 at (Budynas & Nisbett, 2008)

3. EXPERIMENTAL STUDIES AND COMPARISON WITH THEORETICAL MODEL

In experimental studies different kind of rotors and crankshaft are conducted. In experiment test setup rotor and crankshaft are coupled according to serial production method. After that, torque is applied to rotor while crankshaft is fixed. Test setup is shown at Figure 6.

Figure 6: Experimental test setup

Fixing method of crank shaft is not shown in details at Figure 6. In order to fix crank shaft, a mass placed between piston and valve plate. By doing this piston crank mechanism is locked at certain point. For this study eight different compressor models are analyzed. Ten tests are performed for each compressor model in order to gain accurate data. Those compressor models have different crankshaft diameter, rotor outer diameter, interference value and length of interference fit. All of these dimensions are parameters for Equation (16).

In experimental test split of torque is measured, split of torque has relation with press fit pressure. Pressure between crank and rotor causes friction forces against applied torque. According to Coulomb dry friction law; friction forces is linear with perpendicular forces on surface. In this case perpendicular forces are press fit forces. However, there is still one unknown at Coulomb friction law, it is friction coefficient. Friction coefficient is depended to characteristic of mated surfaces. In our case all cranks and rotors are assumed to have same surface characteristic in each other. To sum up; although press fit equation does not give friction torque directly, it is linearly related with it. Therefore press fit equation is enough for prediction new designs, and provide eligible method for defining dimensions.

At Table 3 results of experimental work is given. All of these models are tested for serial production at R&D department; furthermore all of them are operating in the field without causing any problem. Determining of safe torque from theoretical calculation is almost impossible. The reason behind is stochastic boundary conditions. Although transmitted torque rotor to system is known, transportation and assembly line condition are random parameters for system. Therefore while designing new parameters for rotor interference; analyzing trusted model's parameters is beneficial.

Table 3: Experimental results of different compressor models

Model	A	B	C	D	E	F	G	H
Diameter of Crank (mm) r_f	14.0	14.0	16.1	12.0	12.0	13.0	12.0	12.0
Hole Diameter of Crank (mm) r_{ci}	5.5	5.5	6	4.95	4.95	5.5	4.95	4.95
radius value for center of hole (mm) r_{ic}	1.17	1.17	1.3	1.29	1.22	0.81	1.29	1.29
Inner diameter of rotor (mm) r_f	14.0	14.0	16.1	12.0	12.0	13.0	12.0	12.0
Outer Diameter of Rotor (mm) r_{ro}	60.4	60.4	60.4	55.4	55.4	55.4	55.4	55.4
Poisson Ratio for Crank ϑ_c	0.22	0.22	0.22	0.22	0.22	0.22	0.22	0.22
Poisson Ratio for Rotor ϑ_r	0.28	0.28	0.28	0.28	0.28	0.28	0.28	0.28
Modulus of Elasticity for Crank (N/mm^2) E_c	20680 0	206800	206800	206800	206800	206800	206800	206800
Modulus of Elasticity for Rotor (N/mm^2) E_r	12000 0	120000	120000	120000	120000	120000	120000	120000
Angular Velocity (rad/s) ω	314.16	314.16	314.16	314.16	314.16	314.16	314.16	314.16
Average of measured torque (N.m) T	50.567	60.94	90.63	71.08	92.21	92.95	46.233	53.444
Standard deviation of measured torque	12.955	12.491	11.4	5.117	5.6274	10.044	6.4465	6.0711

While applying theoretical model to compressor models, few assumptions are made. Lubrication hole at cranks has angle with main bearing axis. This value varies 1 to 2 degrees in our model. The first assumption is lubrication hole axis and crank main bearing axis are assumed to parallel lines. In theoretical model pressure is function of angle θ, after solving Equation (16) average pressure is calculated from pressure function. After that average pressure is multiplied by area of the interference fit. The rsult is total force acting on crankshaft. In reality this values has to be multiplied by coefficient of friction. Later it has to be multiplied by radius in order to find required torque for split off. In this calculation coefficient of friction is taken as one, for convince. The result of theoretical model is given at Table 4

Table 4: Theoretical results of different compressor models

Model	A	B	C	D	E	F	G	H
Press fit pressure ($x10^7 N/m^2$)	6.161	6.161	6.056	9.501	9.501	6.480	9.501	9.501
Total torque (N.m)	169.84	160.37	208.51	182.85	225.78	166.36	156.03	123.83
Total torque with zero angular velocity (N.m)	170.51	161.00	209.35	183.24	226.26	166.87	156.36	124.10

In above table two torque values are given; one is stationary case which is simulation for transporting conditions, the other is crank rotates at constant speed (3000 rpm) which is simulation for working condition. As it seen from Table 4 zero velocity case and constant speed case is nearly the same. However experiments are conducted at zero velocity case, therefore comparison of experimental result is made with zero velocity case. For comparison graphic is illustrated at Figure 7. Compressor models are sorted smallest to largest according to their experimental split off torque value; these values are represented at x axis of the chart. Y axis of chart represents theoretical value split off torque. Although some compressor models do not verify the theoretical calculations, general tendency of experimental results are similar with theoretical model.

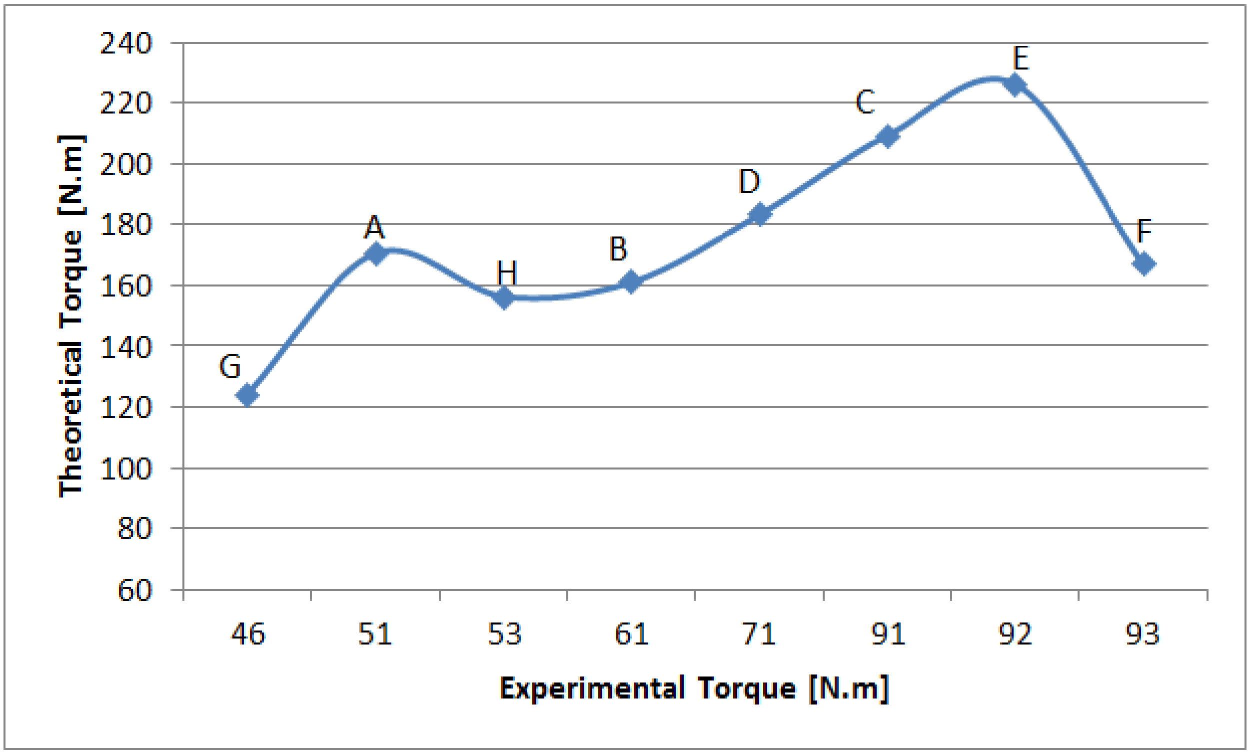

Figure 7: Comparison of experimental and theoretical values

However theoretical model gives more accurate results for crankshafts with same diameter. The line at Figure 8 is almost linear which shows there is a linear relation between theoretical and experimental model.

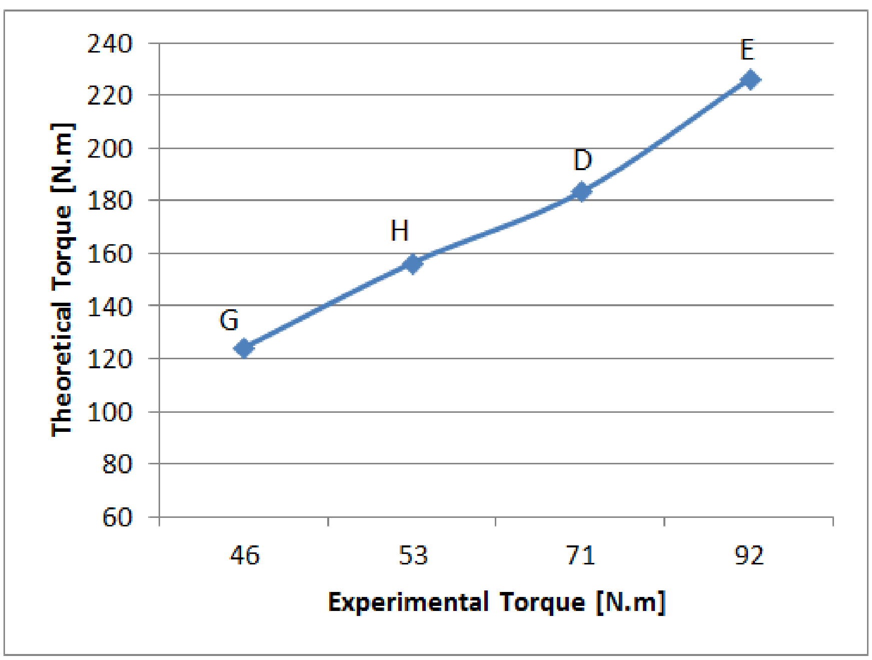

Figure 8: Comparison of experimental and theoretical values

3. CONCLUSION

In this study interference fit between rotor and crankshaft at hermetic compressor is analyzed. Although experiments are conducted for hermetic compressors; method of the experiment and theoretical calculations could be applied any mechanism which contains interference fit. According to this study the following conclusion can be obtained:

- For different crankshaft diameters, there is difference between theoretical and experimental results. However it is consistent for crankshaft with same diameter. The reason behind this may be different end conditions, which do not take account in theoretical calculations, for different crankshaft.
- There can be plastic deformation at crankshaft which is faced with bigger press fit pressure. Therefore this parameter has to take account when designing new models. Furthermore pressure on crankshaft is hard to determine by experimental methods.
- Interference fit value has a biggest influence on split off torque. However as it is said above, it can cause plastic deformation at crankshaft.
- Length of the interference fit has a linear relation with split off torque. Since split off torque is equal to multiplying of pressure and press fit area.
- According to this study; interference fit length of some compressor can shorten up to 4-5 mm without taking any extra risk for field.

This study will be extended with respect to following points

- Theoretical model is analyzed and optimized in order to fit real conditions better
- Experimental studies are continuing, and it will cover all of our compressor models.
- In experimental studies surface roughness and other tolerance values will be measured. Relation between tolerances and will be investigated**.**
- FEM analyses are studied for interference fit phoneme.

NOMENCLATURE

r	radius for polar coordinate	(mm)
θ	angle for polar coordinate	(rad)
z	axial direction	(mm)
σ	stress	(N/mm^2)
ϑ	passion ratio	-
ρ	density	(kg/mm^3)
ω	radial velocity	(rad/sec)
m	mass	(kg)
E	modulus of elasticity	(Pa)
u	displacement	(mm)
δ	radial interference	(mm)
p	press fit pressure	(N/mm^2)
T	Torque	(N.m)

Subscript

r	radial direction
θ	tangential direction
i	inner member
o	outer member
rr	radial direction for rotor
θr	tangential direction for rotor
rc	radial direction for crank
θc	tangential direction for crank
ro	outer of rotor
ci	inner of crank
f	final

REFENCES

Budynas, R. G. (1999). Advanced Strength and Applied Stress Analysis. New York: McGraw-Hill, P. 349
Budynas & Nisbett(2008). Shigley's Mechanical Engineering Design. New York: McGraw-Hill, P. 110

ACKNOWLEDGEMENTS

I would like to thank my colleagues and managers for encouraging me to write this paper at the beginning of my study.